JOURNAL OF GUIDANCE, CONTROL, AND DYNAMICS
Vol. 33, No. 2, March–April 2010

Nonlinear Path Following Method

David J. Gates*
Commonwealth Scientific and Industrial Research Organization, Canberra, Australian Capital Territory, 2601, Australia

DOI: 10.2514/1.46679

This paper develops a new guidance logic for a vehicle to converge to a specified, desired path of general shape in three dimensions. Conditions are found that ensure exponential convergence to the path for any initial vehicle position and velocity vector, excluding only the velocity vector normal to the desired path. The guidance logic includes a ghost vehicle that follows the desired path. The command accelerations are derived from fictitious forces that act in a frame of reference that moves with the ghost. The forces comprise a springlike force between vehicle and ghost and a drag force created by a fictitious medium that moves with the ghost. The motion of the ghost is determined indirectly by a nonlinear constraint that controls the real vehicle speed and leads to a differential-algebraic system of equations. The path equations are formulated in terms of differential geometry, in which time is replaced by distance along the vehicle path. The geometric equations are transformed into standard form differential equations. These are transformed again into kinetic equations for both a fixed medium and a moving medium. The transformed equations provide more explicit formulas for command accelerations and are used to ensure that commands do not exceed the capabilities of the vehicle. Often, the vehicle limitation is more constraining than the convergence conditions. Simulations of a miniature aircraft, using these equations, illustrate the effectiveness of the method. Other methods are compared.

Nomenclature

$\mathbf{e}_P$	=	tangent unit vector to desired path
$\mathbf{F}$	=	effective force on vehicle in frame of reference of ghost, m/s^2
$\bar{\mathbf{F}}$	=	part of curvature vector of vehicle path, m^{-1}
$\mathbf{r}$	=	position vector of vehicle, m
$\mathbf{r}_D$	=	position vector of vehicle relative to ghost, m
$\mathbf{r}_P$	=	position vector of ghost, m
s	=	distance along desired path, m
t	=	time, s
$\mathbf{U}$	=	velocity vector of vehicle relative to medium, m/s
U	=	speed of vehicle relative to medium, m/s
$\mathbf{u}$	=	tangent vector to vehicle path
$\mathbf{u}_P$	=	velocity vector of ghost for unit vehicle speed
$\mathbf{V}$	=	velocity vector of vehicle, m/s
V	=	speed of vehicle, m/s
$\mathbf{W}$	=	velocity vector of wind, m/s
W	=	speed of wind, m/s
w	=	speed of ghost, m/s
ζ	=	ratio of speed of ghost to speed of vehicle
θ, ϕ	=	spherical polar angles of vehicle velocity vector, rad
κ	=	curvature of vehicle path, m^{-1}
κ_P	=	curvature of desired path, m^{-1}
λ	=	rate constant, s^{-1}
μ	=	parameter in vehicle path curvature, m^{-1}
σ	=	distance along vehicle path, m
$\mathbf{\Omega}_D$	=	angular velocity vector of link, rad/s

I. Introduction

THE essence of the path tracking (or path following) problem, in its simplest form, may be stated as follows: devise a simple real-time guidance law that will cause an ideal vehicle to converge to a defined path. The defined path is a general space curve, satisfying suitable smoothness conditions. Convergence is required for a suitably large set of initial conditions. The speed of the vehicle is not to be constrained by the guidance law but controlled independently; the simplest case being constant speed. This problem has proved to be quite challenging and continues to be a topic of research. Potential applications include the safe operation of ships and aircraft.

The guidance equations specify command accelerations that are applied to the vehicle. The present paper is concerned only with this outer-loop guidance. There are well-researched inner-loop methods [1] for implementing these commands in the vehicle. Alternative methods (not studied here) have been developed for combining the inner and outer loops [2–5], but these are usually more complex to use in real applications. In either method, the vehicle needs continuous accurate information about its position and velocity, which might be provided by an inertial navigation system (INS) and the Global Positioning System (GPS).

The traditional method for path following is based on a proportional-integral-derivative (PID) linear controller. This is effective for small deviations in distance or heading from straight defined paths. For aerial vehicles, it is important to allow for the effects of wind. The traditional method has no intrinsic wind compensation. It continually tries to counteract tracking errors caused by the wind, but recent methods perform better on curved paths. The nonlinear method of [6] can accommodate large deviations from straight paths between waypoints.

Another approach is to construct a vector field associated with each part of a defined path [7,8]. The method compensates naturally for wind. Fields have been constructed for tracking a straight path and a circle, in planar motion. Global convergence is proved in these cases, but limits on the turning capability of the vehicle are not included in the proofs. To track toward a path consisting of straight lines and arcs of circles, fields are switched on and off. Paths in the shape of a figure eight require multivalued fields. It is also complicated to construct fields suitable for general defined paths.

Another approach involves following an imaginary point on the desired path [9–13]. A recent version [14–16] of this method has appealing simplicity and provides tight tracking to straight paths and circles for planar motion. The guidance logic is based on ground speed (inertial speed) and compensates naturally for wind. The proof of convergence in [16] allows for limitations on the turn radius of the vehicle. However, if the vehicle is at a distance greater than the circle

Received 10 August 2009; revision received 13 October 2009; accepted for publication 25 October 2009.

*Research Scientist, Optimisation in Air Transport Management Team, Mathematical and Information Sciences, General Post Office Box 664; david.gates@csiro.au.

radius, it does not converge to the circle. Guidance does not exactly track the transition between a straight path and a circle and does not converge exactly to paths of other shapes. Tracking is usually close for general defined paths and, for many purposes, it might be satisfactory. The performance of traditional methods is also illustrated in [14].

The guidance logic presented here overcomes some of the limitations mentioned. It is equally applicable to all three-dimensional (3-D) smooth defined paths. Convergence can be proved under fairly general conditions. A moving medium does not influence the vehicle path, relative to the fixed earth frame, within the natural physical limits. Turning capabilities of the vehicle are accommodated in a simplified way. Like the method of [14–16], it involves a moving reference point on the defined path. The motion of this reference point, or ghost vehicle, is coupled to the motion of the real vehicle by a fictitious mechanical link. In [14–16], this link has fixed length. In the new logic, the link is springlike and supplemented by a fictitious drag force.

The desired path might be constructed by simple empirical rules and might comprise circular arcs and straight paths. Current research uses the mathematical methods of optimal control theory to plan safe energy-efficient paths for aircraft [17–19] and spacecraft [20,21]. These methods do not control the vehicle but can be supplemented by path-following guidance of the type described here.

The paper is organized as follows. Section II defines the new guidance logic. Section III describes the relative motion of the vehicle and the ghost. Section IV formulates convergence in terms of this relative motion. Sections V, VI, and VII obtain initial conditions and rate parameter values that ensure convergence. Section VIII provides a simple analysis of tracking to a circle in planar motion. Section IX gives the geometric equations of the vehicle path in standard differential form. Section X estimates the rate parameter values consistent with vehicle maneuver capabilities by analyzing the curvature of the path. Section XI gives the kinetic guidance equations in standard form for a fixed or moving medium. Section XII gives conclusions and discusses extensions. The paper follows the convention from kinematics, for which the velocity is a vector and the speed is the magnitude of the vector.

II. Guidance Logic

As mentioned, the vehicle speed should not be determined by the guidance logic but chosen independently. This is achieved here by first defining the vehicle path Q geometrically. Then, the vehicle motion is superimposed on Q. Different vehicle speeds, including variable speeds, can thus be superimposed on the same Q. Some resulting equations of motion are given in Sec. XI, but before that, the description is essentially geometric.

The purpose of the guidance logic is to generate a Q that converges toward and ultimately coincides with a specified 3-D path P. Let P be a rectifiable curve parameterized by its local position vector $\mathbf{r}_P(s)$, where s is the distance along P. The curve Q is also required to be rectifiable and is parameterized by its local position vector $\mathbf{r}(\sigma)$, where σ is the distance along Q. With every σ, one associates an $s(\sigma)$ (which will be defined), and so every point on Q has an associated point on P. Such points are said to be linked, and $\mathbf{r}_P[s(\sigma)]$ is called the reference point, corresponding to $\mathbf{r}(\sigma)$. Formally, the objective is to construct a Q such that

$$|\mathbf{r}(\sigma) - \mathbf{r}_P[s(\sigma)]| \to 0 \tag{1}$$

as $\sigma \to \infty$. This implies that, under suitable smoothness conditions, the tangent vectors to the paths also converge, and so Q merges with P asymptotically. Then, a vehicle moving forward on Q will ultimately follow P. The geometric definition of Q in Sec. II.A might appear somewhat abstract. However, it is motivated by kinetic concepts, which are described in Sec. II.B.

A. Geometric Definition of Q

The shape of a space curve is completely defined by specifying its curvature vector [22] at every point on the curve. A derivative with respect to σ is denoted by an overdot, and a derivative with respect to s is denoted by a prime ($'$). In the new guidance logic, Q is defined by the curvature vector:

$$\ddot{\mathbf{r}} = \bar{\mathbf{F}} + \ddot{\mathbf{r}}_P \tag{2}$$

where

$$\bar{\mathbf{F}} = -\mu^2 \mathbf{r}_D - 2\mu \dot{\mathbf{r}}_D \tag{3}$$

The deviation $\mathbf{r}_D = \mathbf{r} - \mathbf{r}_P$ is the relative position of the linked points, and $\mu > 0$ is a parameter affecting the rate of convergence. One can write $\dot{\mathbf{r}}_D = \mathbf{u} - \mathbf{u}_P$, where $\mathbf{u} = \dot{\mathbf{r}}$ is the unit vector along the forward tangent to Q, and

$$\mathbf{u}_P = \dot{\mathbf{r}}_P = \dot{s}\mathbf{e}_P \tag{4}$$

where $\mathbf{e}_P = \mathbf{r}'_P$ is the unit vector along the forward tangent to P. Equation (2) has 4 degrees of freedom, comprising s and the three components of $\mathbf{r}$, and determines only the relative position of the linked points. However, the requirement that $\mathbf{u}$ be a unit vector imposes an additional constraint:

$$|\mathbf{u}| = 1 \tag{5}$$

This removes the degree of freedom associated with the distance $s(\sigma)$, and so this function is implicitly defined. Then, Q is completely determined by a point and a tangent at a given σ (say $\sigma = 0$). We call this adaptive link (AL) guidance, because the location of the reference point is not specified directly but must adapt so as to satisfy Eq. (5).

Equations (2) and (5) form a nonlinear differential-algebraic system, with state variables $\mathbf{r}$, $\mathbf{u}$, and s. It is possible to solve these equations by numerical methods [23], but they will be transformed into ordinary differential equations (Sec. IX), for which the numerical solution is much simpler.

Equation (2) may be written as

$$\ddot{\mathbf{r}}_D + 2\mu \dot{\mathbf{r}}_D + \mu^2 \mathbf{r}_D = \mathbf{0} \tag{6}$$

which resembles proportional and derivative (PD) control [14,16]. The constraint in Eq. (5) means that the guidance differs markedly from typical PD guidance [14], which is designed to converge to a straight P, with Q nearly parallel to P. The present guidance logic allows any direction for Q, with the single exception of the normal to P, as will be shown. However, Eq. (5) greatly complicates the equations and the analysis of convergence.

We consider a class of P, for which $\mathbf{e}_P(s)$ is continuous, called continuously differentiable curves [24]. Equation (2) involves the curvature vector $\mathbf{e}'_P$ of P [22], but we do not require that this derivative exists (i.e., be continuous) everywhere. Rather, we require that in any finite interval (of fixed length), the derivative exists, except at a finite number of points or values of s. (The fixed length condition is to ensure that intervals do not become arbitrarily small as $s \to \infty$ in open curves of infinite length.) At the exceptional points, we require that the one-sided derivatives exist, where $\mathbf{e}'_P$ is interpreted as a left or right derivative; the choice does not matter. This admits, for example, a path that leaves a circle on a straight line tangent, for which $\mathbf{e}'_P$ is discontinuous at the point of tangency.

We also suppose that $\mathbf{e}'_P$ is bounded and possesses only a finite number of maxima and minima on finite intervals of values s of fixed length. These Dirichlet conditions imply that the Riemann integral of $\mathbf{e}'_P$, namely $\mathbf{e}_P$, exists and is therefore continuous, as specified previously. This is an essential condition for Theorem 1. Incidentally, the conditions also imply that, on intervals of P, $\mathbf{e}'_P$ can be represented by a Fourier series that converges (pointwise) to $\mathbf{e}'_P$ at points s of continuity [24]. More general paths can be accommodated, such as an $\mathbf{e}'_P$ of bounded variation [24], but the class of paths chosen is more than adequate for this application.

In practice, the achievable curvature κ of Q will be limited by the vehicle maneuverability, with the limitation depending on the type of vehicle, the speed of the vehicle, the type of maneuver, and the

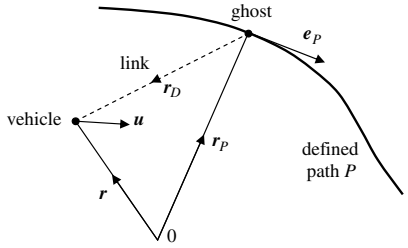

Fig. 1 Sketch of the vehicle motion and the defined path.

medium. The effects of constraints on κ are studied in Sec. X. Although a real vehicle will not be able to change its κ discontinuously, this smaller effect is not considered here.

B. Kinetic Interpretation

The path Q has been defined by differential equations, with σ as the independent variable. Thus, Q is a space curve defined by its differential geometry. The definition might seem rather formal and, perhaps, somewhat obscure. However, the equations are motivated by kinetic concepts, and the ideas become clearer if cast in these terms. This is done by considering a vehicle moving with a unit speed along Q. Then, σ is also the time expired. Likewise, we consider a ghost vehicle at $\mathbf{r}_P$ moving along P, as sketched in Fig. 1. Then, $s(\sigma)$ is the distance travelled by the ghost at time σ. Now, $\mathbf{u}$ is interpreted as the velocity vector of the vehicle, $\mathbf{u}_P = \dot{s}\mathbf{e}_P$ is the velocity of the ghost, and $\dot{s}$ is its speed. Also, $\dot{\mathbf{r}} = \dot{\mathbf{u}}$ is interpreted as the command acceleration on the vehicle. Equation (5) implies that the acceleration $\dot{\mathbf{u}}$ is purely lateral, and produces only turning, in any plane. Equivalently, the vehicle has a notional unit mass and is driven by the Newtonian Eq. (2). This implies that, in a frame of reference that moves with the ghost, the vehicle feels a total force $\bar{\mathbf{F}}$, comprising a spring force $-\mu^2\mathbf{r}_D$ directed toward the ghost and a drag force $-2\mu\dot{\mathbf{r}}_D$ directed along the relative velocity. The latter can be interpreted as arising from a fictitious medium moving with the ghost, exerting a drag force on the vehicle, proportional to the speed of the vehicle relative to the medium. This is intuitively right, because the vehicle should ultimately be stationary in this frame of reference and feel no spring force or drag force. Thus, the steady-state solution is $\mathbf{r}_D = \mathbf{0}$, for which the defined path is achieved and $\bar{\mathbf{F}} = \mathbf{0}$.

As mentioned, the equations represent a generalized form of PD control. In a standard PD controller, centrifugal force causes the vehicle to track wide on a turn (Fig. 11a in [14]). In the new method, reference to the moving frame removes the centrifugal force.

C. Steady States

In a steady state of AL guidance or, equivalently, a geometric solution where Q coincides with P, Eq. (6) implies that $\dot{\mathbf{r}}_D = \mathbf{0}$, and so $\mathbf{u} = \dot{s}\mathbf{e}_P$. As $\mathbf{u}$ and $\mathbf{e}_P$ are unit vectors, there are two steady states, $\{\dot{s} = 1,\ \mathbf{u} = \mathbf{e}_P\}$ and $\{\dot{s} = -1,\ \mathbf{u} = -\mathbf{e}_P\}$, corresponding to the forward and backward tracking of P, respectively. The existence of two steady states complicates the convergence theory. Even if P is closed, there must be two limit cycles in the state space and regions of instability between them. The main task is to determine which of these two steady states is achieved from which initial states, and under what conditions.

III. Relative Motion of Vehicle and Ghost

Having provided the kinetic interpretation, we shall continue to use it, although bearing in mind that the formulation is really geometric. Analysis of AL guidance begins by studying the relative motion of the vehicle and the ghost, determined by Eq. (6) alone. This equation has some simple consequences. It implies that any component of $\mathbf{r}_D$ behaves like a simple, critically damped oscillator. Its solution has the form

$$\mathbf{r}_D = (\mathbf{A} + \mathbf{B}\sigma)\exp(-\mu\sigma) \tag{7}$$

where $\mathbf{A}$ and $\mathbf{B}$ are constant vectors determined by initial values of $\mathbf{r}_D$ and $\dot{\mathbf{r}}_D$. This implies that $\mathbf{r}_D$ remains confined to the plane of fixed orientation, containing $\mathbf{A}$ and $\mathbf{B}$ for any 3-D motion. Also,

$$-(\log|\mathbf{r}_D|)/\sigma = \mu - (\log|\mathbf{A} + \mathbf{B}\sigma|)/\sigma = \mu - o(1) \tag{8}$$

as $\sigma \to \infty$, and so $\mathbf{r}_D$ may be said to converge exponentially to zero at rate $\mu - o(1)$, a rate which is slightly less than μ but ultimately infinitesimally close to μ. The angular velocity vector of the link has a magnitude equal to the rotation rate and direction along the axis of rotation in the right-hand sense. It is given by

$$\boldsymbol{\Omega}_D = \frac{\mathbf{r}_D \times \dot{\mathbf{r}}_D}{|\mathbf{r}_D|^2} \tag{9}$$

From Eq. (7),

$$\dot{\mathbf{r}}_D = (\mathbf{B} - \mathbf{A}\mu - \mathbf{B}\mu\sigma)\exp(-\mu\sigma) \tag{10}$$

and so

$$\boldsymbol{\Omega}_D = \frac{\mathbf{A} \times \mathbf{B}}{|\mathbf{A} + \mathbf{B}\sigma|^2} \tag{11}$$

which implies that $\boldsymbol{\Omega}_D \to \mathbf{0}$ as $\sigma \to \infty$. Consequently, the link has a limiting direction, and the convergence is quadratic, not exponential. The angle ψ between $\mathbf{r}_D$ and $\dot{\mathbf{r}}_D$ is given by

$$\sin\psi = \frac{|\mathbf{r}_D \times \dot{\mathbf{r}}_D|}{|\mathbf{r}_D||\dot{\mathbf{r}}_D|} = \frac{|\mathbf{A} \times \mathbf{B}|}{|\mathbf{A} + \mathbf{B}\sigma||\mathbf{B} - \mathbf{A}\mu - \mathbf{B}\mu\sigma|} \tag{12}$$

which tends to zero quadratically. Thus, the direction of the drag force tends quadratically toward the direction of the spring. There are a few other points of interest.

1) According to Eq. (11), the direction of $\boldsymbol{\Omega}_D$ remains fixed, even for nonplanar motion.

2) For coplanar motion, one can choose an initial ghost state $(\mathbf{r}_P, \mathbf{u}_P)$, such that the link direction is constant and $\boldsymbol{\Omega}_D$ is zero. To do this, with a given initial $\mathbf{r}$ and $\mathbf{u}$, one chooses the initial $\mathbf{r}_P$ and $\mathbf{u}_P$, such that $\mathbf{r}_D$ is parallel to $\dot{\mathbf{r}}_D = \mathbf{u} - \mathbf{u}_P$.

3) If $\boldsymbol{\Omega}_D$ is initially zero, it remains fixed at zero, and the direction of the link remains fixed.

Properties 2) and 3) are illustrated for a straight defined path in Secs. V and VI for a circular defined path in Sec. VII and, more generally, at the end of Sec. VII. The properties provide a simple solution method for a circular defined path. The general convergence theory it not limited to a fixed link direction, however.

In the method of [14–16], the link direction changes markedly and sometimes rapidly, as Fig. 17 of [15] shows. Hence, the speed of the ghost can change significantly and differ markedly from the vehicle speed. In AL guidance, the link direction usually changes only slightly, or not at all if the initial conditions are chosen optimally (Secs. V, VI, VII, and VIII). Hence, the motion of the ghost is more uniform and mimics the projection of the vehicle motion on P.

IV. Influence of Relative Motion on Convergence

Conditions for convergence of Q to P will be obtained here (and in subsequent sections) for various types of paths. In the kinetic interpretation, convergence and asymptotic stability are synonymous, but the term stability is not used in the geometric setting. The method used here comprises two distinct steps. The first, studied in this section, is to show how the relative motion (of $\mathbf{r}_D$) affects convergence, in general. The second, studied in later sections, is to control the relative motion. Because $\mathbf{r}_D$ is given by an independent Eq. (6), the second step can be examined independently. It depends on the type of motion and whether the link direction is fixed, as shown in later sections.

A set of states in a kinetic system is said to be invariant if any initial state in the set remains in the set. For example, any first integral (or constant of the motion) defines an invariant set. We consider analogous invariant sets in the differential geometric system of Eqs. (5) and (6). The state vector is denoted as $\boldsymbol{\Xi} = (\mathbf{r},\ \mathbf{u},\ s)$. The set

of states for which Q meets P is $M = \{\Xi\colon \mathbf{r}_D = \mathbf{0}\}$. The steady state with $\dot{s} = 1$ is represented by the invariant set:

$$i_+ = \{\Xi\colon \mathbf{u} = \mathbf{e}_P\} \cap M \tag{13}$$

and the steady state with $\dot{s} = -1$ is represented by the invariant set

$$i_- = \{\Xi\colon \mathbf{u} = -\mathbf{e}_P\} \cap M \tag{14}$$

We also consider the disjoint open sets:

$$I_+ = \{\Xi\colon \mathbf{u} \cdot \mathbf{e}_P > 0\} \tag{15}$$

and

$$I_- = \{\Xi\colon \mathbf{u} \cdot \mathbf{e}_P < 0\} \tag{16}$$

Figure 1 illustrates a state in I_+. Then, $i_+ \subset I_+$ and $i_- \subset I_-$. The method consists of finding conditions under which I_+ and I_- are invariant and contracting into their invariant subsets. One notes the distinction between i_+ (or i_-) and the range or $\mathbf{r}_P(s)$, which is a set in R^3, representing P.

Theorem 1. Suppose that $\mathbf{e}'_P$ satisfies the Dirichlet conditions, and $\mu > 0$ and

$$|\dot{\mathbf{r}}_D| < 1 \tag{17}$$

for all σ. Then, as $\sigma \to \infty$ in AL guidance, initial states in I_+ converge onto i_+, and initial states in I_- converge onto i_-. The convergence is exponential with the rate $\mu - o(1)$. Also, s is strictly increasing in I_+ and strictly decreasing in I_-.

Proof. Equation (4) gives

$$\dot{\mathbf{r}}_D = \mathbf{u} - \dot{s}\mathbf{e}_P \tag{18}$$

and so

$$\dot{\mathbf{r}}_D \times \mathbf{e}_P = \mathbf{u} \times \mathbf{e}_P \tag{19}$$

Using Eq. (17), we therefore get

$$\begin{aligned} |\mathbf{u} \cdot \mathbf{e}_P| &= \sqrt{1 - |\mathbf{u} \times \mathbf{e}_P|^2} = \sqrt{1 - |\dot{\mathbf{r}}_D \times \mathbf{e}_P|^2} \\ &> \sqrt{|\dot{\mathbf{r}}_D|^2 - |\dot{\mathbf{r}}_D \times \mathbf{e}_P|^2} = |\dot{\mathbf{r}}_D \cdot \mathbf{e}_P| \geq 0 \end{aligned} \tag{20}$$

and so $|\mathbf{u} \cdot \mathbf{e}_P| > 0$ for all σ, noting the strict inequality. The Dirichlet conditions imply that $\mathbf{e}_P$ is continuous, and the differential Eq. (2) implies that $\mathbf{u}$ is continuous, and so $\mathbf{u} \cdot \mathbf{e}_P$ is continuous. Then Eq. (20) implies that $\mathbf{u} \cdot \mathbf{e}_P$ cannot change sign, and so I_+ is invariant. The solution in Eq. (7) implies that every state converges to a state of motion on P. The only such states in I_+ are in i_+, and so every state in I_+ converges to i_+. Likewise, every state in I_- converges to i_-.

Equation (7) implies that $(\mathbf{r}, \mathbf{u})$ tends exponentially to $(\mathbf{r}_P, \mathbf{u}_P)$ with the rate $\mu - o(1)$. In I_+, Eq. (20) implies

$$\mathbf{u} \cdot \mathbf{e}_P > \dot{\mathbf{r}}_D \cdot \mathbf{e}_P \tag{21}$$

Thus, Eq. (18) implies

$$\dot{s} = \mathbf{u} \cdot \mathbf{e}_P - \dot{\mathbf{r}}_D \cdot \mathbf{e}_P > 0 \tag{22}$$

and so s increases strictly up to a steady-state asymptote $\sigma +$ constant. We note that $|\dot{\mathbf{r}}_D \times \mathbf{e}_P| \leq |\dot{\mathbf{r}}_D| < 1$ and $1 - |\dot{\mathbf{r}}_D|^2 \leq 1$, and so Eq. (20) implies

$$\mathbf{u} \cdot \mathbf{e}_P \geq \sqrt{1 - |\dot{\mathbf{r}}_D|^2} \geq 1 - |\dot{\mathbf{r}}_D|^2 \tag{23}$$

in I_+. Equation (22) implies

$$\mathbf{u} \cdot \mathbf{e}_P - |\dot{\mathbf{r}}_D \cdot \mathbf{e}_P| \leq \dot{s} \leq \mathbf{u} \cdot \mathbf{e}_P + |\dot{\mathbf{r}}_D \cdot \mathbf{e}_P| \tag{24}$$

With Eq. (23), this implies

$$1 - |\dot{\mathbf{r}}_D| - |\dot{\mathbf{r}}_D|^2 \leq \dot{s} \leq 1 + |\dot{\mathbf{r}}_D| \tag{25}$$

and so $\dot{s}$ converges exponentially to 1 at the rate $\mu - o(1)$. In I_- (similarly) $\dot{s} < 0$, and $\dot{s}$ converges exponentially to -1 at the rate $\mu - o(1)$. This completes the proof. □

The condition $|\dot{\mathbf{r}}_D(0)| < 1$ places restrictions on the initial position and speed of the ghost, such as $\dot{s}(0) > 0$ in I_+ and $\dot{s}(0) < 0$ in I_-. These mean that the initial motion of the ghost is not opposed to the initial motion of the vehicle. During the initial and transient motion, the speed of the ghost can differ significantly from its steady-state value. However, Eqs. (17), (22), and (25) show that the direction and speed of the ghost are well constrained; thus,

$$0 < \dot{s} < 2 \tag{26}$$

in I_+

$$-2 < \dot{s} < 0$$

in I_-. Hence, the ghost cannot reverse its direction on P or move very fast.

The next few sections obtain initial conditions, under which Eq. (17) is satisfied for straight paths P, circular P, and general P. These will provide useful conditions for convergence.

V. Tracking a Straight Path in Planar Motion

This section studies a planar path Q converging to a coplanar straight path P. It provides formulas for Q, and complete conditions for convergence, plus some simple conditions. Here, one takes the x axis along P, and so $\mathbf{r} = (x, y)$, $\mathbf{r}_P = (s, 0)$, and $\mathbf{r}_D = (x - s, y)$, as shown in Fig. 2. The y component of Eq. (6) is

$$\ddot{y} + 2\mu\dot{y} + \mu^2 y = 0 \tag{27}$$

which determines y and shows that the transverse motion is just that of a critically damped oscillator. It implies that the vehicle behaves as though it were connected to P by a critically damped spring that is always normal to P. The components of the vehicle velocity $\mathbf{u}$ are

$$\dot{x} = \cos\theta \tag{28}$$

and

$$\dot{y} = \sin\theta$$

where θ is the angle between $\mathbf{u}$ and P. The second equation determines θ and implies that θ tends exponentially to zero. The first then determines x. Thus, the motion of the vehicle is determined and is independent of the motion of the ghost. One notes that the guidance laws of [7,14–16] do not have such simple solutions in this case.

The x component of Eq. (5) becomes

$$\ddot{s} + 2\mu\dot{s} + \mu^2 s = \ddot{x} + 2\mu\dot{x} + \mu^2 x \tag{29}$$

which shows that the ghost behaves as a critically damped oscillator, with the forcing term given by the known right side. In this case, therefore, the ghost is driven by the vehicle, and the ghost motion is irrelevant. The steady-state solution is $s = x$ and $\dot{s} = 1$, in which the link is parallel to the y axis. For the special case, where $s(0) = x(0)$ and $\dot{s}(0) = \dot{x}(0)$, one gets $s = x$ for all σ, and the link remains parallel to the y axis.

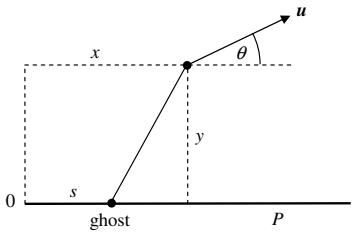

Fig. 2 Coordinates for coplanar guidance to a straight path. The vehicle can lead or lag the ghost.

The condition in Eq. (17) implies $|\dot{y}| < 1$, which Eq. (28) shows to be necessary here, and Eq. (28) ensures that $|\theta| < \pi/2$. This leads to a general convergence condition.

Theorem 2. In AL guidance, a planar path Q converges to the coplanar straight path P if, and only if, $\mu > 0$

$$|\dot{y}(0)| < 1 \tag{30}$$

and

$$|\dot{y}(0) + \mu y(0)| \exp\left[-\frac{2\dot{y}(0) + \mu y(0)}{\dot{y}(0) + \mu y(0)}\right] < 1 \tag{31}$$

Proof. Solving Eq. (27) yields

$$\dot{y} = (B - A\mu - B\mu\sigma)\exp(-\mu\sigma) \tag{32}$$

and

$$\ddot{y} = \mu(-2B + A\mu + B\mu\sigma)\exp(-\mu\sigma) \tag{33}$$

where $A = y(0)$ and $B = \dot{y}(0) + \mu y(0)$. Thus, $\dot{y}$ has a single turning point $\ddot{y} = 0$ at

$$\sigma^* = \frac{2B - \mu A}{\mu B} \tag{34}$$

and then

$$\dot{y}(\sigma^*) = -B\exp(-\mu\sigma^*) \tag{35}$$

If $\sigma^* \geq 0$, then it is necessary that $|\dot{y}(\sigma^*)| < 1$, which is Eq. (31). If $\sigma^* < 0$, then the maximum $|\dot{y}|$ occurs at $\sigma = 0$, where $\dot{y}(0) = -B(1 - \mu\sigma^*)$. Then, $\exp(-\mu\sigma^*) > 1 - \mu\sigma^*$, and so Eq. (30) implies Eq. (31), which completes the proof. □

The maximum value of μ can be obtained by solving Eq. (31) by Newton's method, but simpler conditions can be obtained as follows. Figure 3 shows the set $S(\mu)$ of initial states defined by Eqs. (30) and (31) and the subset where $\sigma^* < 0$. The figure indicates that $S(\mu)$ contains the set $\{\mu|y(0)| \leq 2,\ |\dot{y}(0)| < 1\}$, which provides a simple sufficient condition for convergence as follows.

Corollary 2.a. Suppose that $\mu > 0$, $|\dot{y}(0)| < 1$, and

$$\mu|y(0)| \leq 2 \tag{36}$$

Then, in AL guidance, a planar path Q converges to the coplanar straight path P, as described in Theorem 1.

Remark. Eq. (36) is satisfied for all μ if $|y(0)| = 0$, and so the convergence rate can be arbitrarily large.

Proof. The conditions comprise two sets: $S_+ = \{B > 0,\ \mu A \leq 2\}$ and $S_- = \{B < 0,\ -2 \leq \mu A\}$. In S_+, Eq. (34) implies $\sigma^* \geq 2x/\mu$, where $x = 1 - 1/B$. If $\sigma^* \leq 0$, then Eq. (30) suffices for convergence. If $\sigma^* > 0$, there are two cases. The first is $B \leq 1$, where Eq. (35) implies $0 > \dot{y}(\sigma^*) > -1$. The second is $B > 1$. We also have $B \leq |\dot{y}(0)| + \mu|y(0)| < 3$, and so $0 < x < 2/3$ in this case. Then, Eq. (35) gives

$$0 > \dot{y}(\sigma^*) \geq -B\exp(-2 - 2/B) = -e^{-2x}/(1 - x) > -1 \tag{37}$$

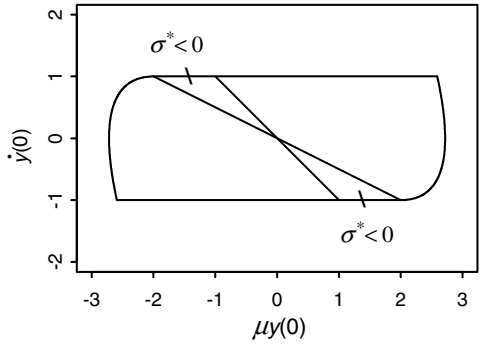

Fig. 3 The convergent set $S(\mu)$.

In S_-, the case $\sigma^* \leq 0$, and the case where $\sigma^* > 0$ and $B > -1$ are again trivial. Otherwise, $-3 < B < -1$, which implies similarly that $0 < \dot{y}(\sigma^*) < 1$. This completes the proof. □

Figure 3 indicates that $S(\mu)$ is contained by the set $\{|\dot{y}(0)| \leq 1\}$ and by the set $\{\mu|y(0)| \leq e\}$, which provide simple necessary conditions for convergence as follows.

Corollary 2.b. In AL guidance, a planar path Q does not converge to a coplanar straight path P if $|\dot{y}(0)| > 1$ or

$$\mu|y(0)| > e \tag{38}$$

Proof. Convergence fails if $|\dot{y}(0)| > 1$, by Theorem 2. If $|\dot{y}(0)| \leq 1$ and $\mu A > e$, then $B > -1 + e > 0$. Hence, $\sigma^* < 2z/\mu$, where $z = 1 - e/(2B) < 1$, and so

$$\dot{y}(\sigma^*) < -e^{1-2z}/(2 - 2z) \leq -1 \tag{39}$$

(with equality at $z = 1/2$ only). If $\mu A < -e$, then similarly $\dot{y}(\sigma^*) > 1$, which completes the proof. □

If μ is too large, then the vehicle is driven into the boundary set:

$$I_0 = \{\Xi\colon \mathbf{u} \cdot \mathbf{e}_P = 0\} \tag{40}$$

between I_+ and I_-. Then, the curvature of Q becomes infinite, and the paths fail to converge.

Figure 4 illustrates the solution for which Q starts at coordinates (0, 100) at an angle of $\theta = 60$ deg with the x axis. The ghost starts at the origin (0, 0), with $\dot{s} = 0.5$ to maintain a fixed link direction. Theorem 2 shows that convergence will occur if $\mu = 0.026$ m^{-1} but not if $\mu = 0.027$ m^{-1}. The value 0.024 is used in Fig. 4, which confirms the convergence. Park et al. [14] consider a vehicle speed of 25 m/s, which would imply a convergence rate of $25\mu = 0.6$ s^{-1} or a time constant of $1.\dot{6}$ s, which is very fast. Section X illustrates how such solutions are influenced by limitations on the turn radius of the vehicle.

In the method of [14–16], Eq. 4 of [14] shows that guidance ultimately converges exponentially at the rate $\mu = \sqrt{2}/L_1$, where L_1 is the fixed length of the link. There is a small oscillation toward convergence, because the asymptotic motion is slightly underdamped. The constraint $L_1 > |y(0)|$ implies $\mu < \sqrt{2}/|y(0)|$, which is smaller than the rate admitted by Eq. (31); and Eq. (36) admits a larger rate still. However, limitations on the vehicle turning rate sometimes confine μ to smaller values (Sec. X).

VI. Tracking a Straight Path in Nonplanar Motion

This section studies a nonplanar path Q converging to a straight path P. It provides formulas for Q, and some strong (but incomplete) conditions for convergence. Here, one takes the x axis along P, and so $\mathbf{r} = (x, y, z)$, $\mathbf{r}_P = (s, 0, 0)$, and $\mathbf{r}_D = (x - s, y, z)$. The y component of Eq. (6) is again Eq. (27), and the z component is

$$\ddot{z} + 2\mu\dot{z} + \mu^2 z = 0 \tag{41}$$

which determines y and z, The components of the tangent vector $\mathbf{u}$, or of the vehicle velocity vector, may be written in the form

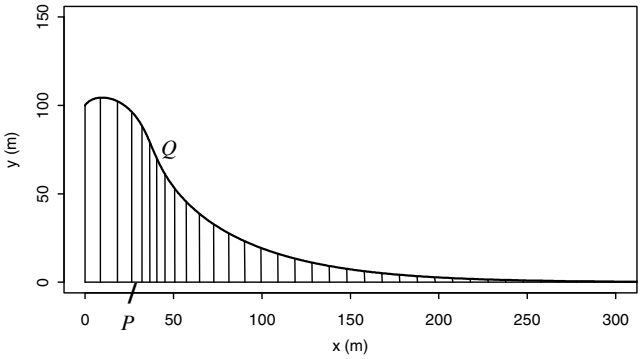

Fig. 4 An example of coplanar convergence of a vehicle to a straight path, with some links shown at equal intervals along the vehicle path.

$$\dot{x} = \cos\theta, \qquad \dot{y} = \sin\theta\cos\phi, \qquad \dot{z} = \sin\theta\sin\phi \tag{42}$$

where θ and ϕ are the spherical polar angles of $\mathbf{u}$. The last two equations determine θ and ϕ, and the first then determines x. The radius vector, normal to the defined path, is $\mathbf{r}_N = (0, y, z)$. Then, Theorem 1 and Eq. (42) show that the path converges if, and only if, $|\dot{\mathbf{r}}_N(\sigma)| < 1$ for all σ. As in the planar case, this can be reduced to conditions on the extreme values of $|\dot{\mathbf{r}}_N(\sigma)|$, which can be related to initial conditions. General conditions analogous to Theorem 2 are rather cumbersome. More convenient, but incomplete, conditions are generalizations of Corollaries 2.1 and 2.2 as follows.

Theorem 3. Suppose that $\mu > 0$, $|\dot{\mathbf{r}}_N(0)| < 1$, and

$$\mu|\mathbf{r}_N(0)| \le 2 \tag{43}$$

Then, in AL guidance, a path Q converges to the straight defined path P, as described in Theorem 1.

Proof. We choose the Y axis, so as to bisect the angle (2α, say) between $\mathbf{r}_N(0)$ and $\dot{\mathbf{r}}_N(0)$, as illustrated in Fig. 5. Then,

$$|\dot{y}(0)| = |\dot{\mathbf{r}}_N(0)|\cos\alpha < \cos\alpha \tag{44}$$

Also, $|y(0)| = |\mathbf{r}_N(0)|\cos\alpha$, and so Eq. (43) can be written as

$$\mu|y(0)| \le 2\cos\alpha \tag{45}$$

Corollary 2.a., with Eqs. (44) and (45), implies $|\dot{y}| < \cos\alpha$ for all σ. By the same argument, one obtains $|\dot{z}| < \sin\alpha$ for all σ. As $|\dot{\mathbf{r}}_N|^2 = |\dot{y}|^2 + |\dot{z}|^2$, it follows that $|\dot{\mathbf{r}}_N| < 1$ for all σ. Theorem 1 then implies convergence. □

Theorem 4. In AL guidance, a path Q does not converge to the straight defined path P if $|\dot{\mathbf{r}}_N(0)| > 1$ or

$$\mu|\mathbf{r}_N(0)| > e \tag{46}$$

Proof. Choose the y axis parallel to $\mathbf{r}_N(0)$. Then, Eq. (46) becomes Eq. (38), and Corollary 2.b. implies $|\dot{y}(\sigma^*)| > 1$, which implies no convergence. □

One notes that Theorems 3 and 4 do not provide complete conditions for convergence, because the interval $2 < \mu|\mathbf{r}_N(0)| \le e$ is not covered. Figure 6 illustrates the solution, for which Q starts on the z axis at coordinates $\mathbf{r}(0) = (0, 0, 100)$ m in the (x, y) plane and makes an angle of 60 deg with the x axis, and so $\mathbf{u}(0) = (1/2, \sqrt{3}/2, 0)$. The ghost starts at the origin with $\dot{s} = 0.5$ to maintain a fixed link direction. Theorem 3 shows that convergence will occur if $\mu = 0.02$ m^{-1}. This is used in Fig. 6, which confirms the convergence, and illustrates the nonplanar motion of the vehicle. Park et al. [14] consider a vehicle speed of 25 m/s, which would imply a convergence rate of $25\mu = 0.5$ s^{-1}, or a time constant of only 2 s. Again, Sec. X illustrates how such solutions are influenced by limitations on the turn radius of the vehicle.

VII. Convergence to Curved Three-Dimensional Defined Paths

Here, we give conditions for convergence to a general 3-D defined path.

Theorem 5. Suppose that $\mathbf{e}'_P$ satisfies the Dirichlet conditions, and $\mu > 0$, $|\dot{\mathbf{r}}_D(0)| < 1$, and

$$\mu|\mathbf{r}_D(0)| \le 2 \tag{47}$$

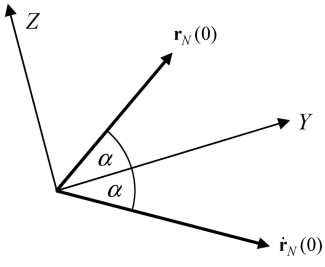

Fig. 5 Choice of coordinate axes in the proof of Theorem 3.

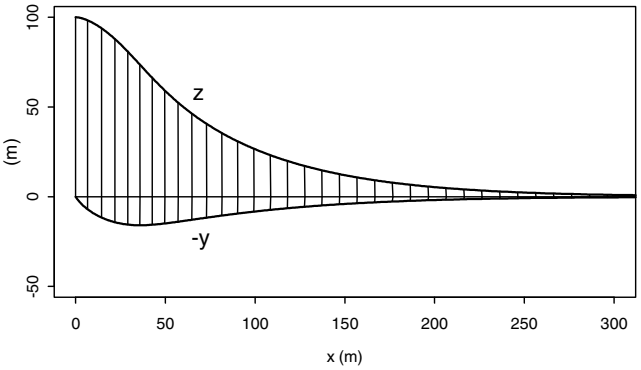

Fig. 6 An example of nonplanar convergence of a vehicle to a straight path, with some links shown at equal intervals along the vehicle path.

Then, in AL guidance, path Q converges to path P, as described in Theorem 1.

Proof. As described in Sec. III, $\mathbf{r}_D$ is confined to a plane (of fixed orientation). In this plane, one chooses orthogonal axes Y and Z, of a fixed direction, and one writes $\mathbf{r}_D = (y_D, z_D)$ with components relative to these axes. Then, Eq. (6) becomes

$$\ddot{y}_D + 2\mu\dot{y}_D + \mu^2 y_D = 0, \qquad \ddot{z}_D + 2\mu\dot{z}_D + \mu^2 z_D = 0 \tag{48}$$

Using the method of Theorem 3, one obtains the proof. □

It is notable that the conditions do not depend explicitly on the shape of the defined path, though the orientation of the defined path at the initial ghost position influences the initial value of $\dot{s}$ via the constraint on $|\dot{\mathbf{r}}_D(0)|$. Comparison of Eq. (43) with Eq. (47) shows that Theorem 3 is stronger than Theorem 5 for a straight path, because $|\mathbf{r}_N| \le |\mathbf{r}_D|$. The Theorems coincide only if the chosen plane is normal to the straight path.

The condition in Eq. (47) shows that a vehicle can track to any path from an arbitrarily large distance $|\mathbf{r}_D(0)|$ by choosing a small enough μ. In practice, this could produce slow convergence, and so it would be more practical to steer toward the path and initiate guidance only when a suitably large μ is possible. Because $|\mathbf{r}_D| \to 0$ as $\sigma \to \infty$, one can subsequently accelerate convergence by choosing a larger μ consistent with Eq. (47).

One can choose the initial ghost position and speed so as to maximize the convergence rate. First, Eq. (47) shows that μ can be maximized if $|\mathbf{r}_D(0)|$ is minimized. The latter is achieved if the ghost is initially located on the normal to the path through $\mathbf{r}(0)$, so that

$$\mathbf{r}_D(0) \cdot \mathbf{e}_P(0) = 0 \tag{49}$$

Convergence can be further improved by choosing an optimal initial $\dot{s}$. From Eq. (7), we have $|\mathbf{r}_D|^2 = q\exp(-2\mu\sigma)$, where $q = |\mathbf{A} + \sigma\mathbf{B}|^2$, $\mathbf{A} = \mathbf{r}_D(0)$, and $\mathbf{B} = \mu\mathbf{r}_D(0) + \dot{\mathbf{r}}_D(0)$. Using Eqs. (18) and (49), one gets $q = q_1 + \sigma^2 q_2$, where

$$q_2 = |\mathbf{u}(0) - \dot{s}(0)\mathbf{e}_P(0)|^2 \tag{50}$$

and q_1 does not involve $\dot{s}(0)$. A variation of q_2, with respect to $\dot{s}(0)$, shows that q_2 is minimal if

$$\dot{s}(0) = \mathbf{u}(0) \cdot \mathbf{e}_P(0) \tag{51}$$

Thus, the component of velocity of the vehicle, parallel to P, initially equals the speed of the ghost. The result is summarized as follows.

Theorem 6. In AL guidance, under the conditions of Theorem 5, the highest rate of convergence is achieved if the initial ghost position and speed satisfy Eqs. (49) and (51).

The latter conditions imply that $\dot{\mathbf{r}}_D(0)$ and $\mathbf{B}$ are normal to $\mathbf{e}_P(0)$. Hence, $\mathbf{r}_D$ (and consequently $\dot{\mathbf{r}}_D$) are confined to the plane normal to $\mathbf{e}_P(0)$ for all σ. Equivalently, Eq. (9) implies that $\boldsymbol{\Omega}_D$ remains parallel to $\mathbf{e}_P(0)$. Examples are given in Sec. IX. For coplanar motion, $\mathbf{r}_D$ and $\dot{\mathbf{r}}_D$ remain parallel to $\mathbf{r}_D(0)$, and $\boldsymbol{\Omega}_D = \mathbf{0}$. The examples of Sec. V and VIII illustrate this.

There is no simple analogue of Theorem 4, giving necessary conditions for convergence, because the shape of the defined path is involved in a complex way. The next example illustrates this.

VIII. Tracking a Circle in Planar Motion

Here, we study planar tracking to a circular path. The initial ghost conditions are chosen optimally, according to Theorem 6, producing a fixed link direction. Then, Eqs. (5) and (6) simplify, and more explicit detail can be obtained. For the geometry in Fig. 7, the link direction is taken along the x axis without loss of generality.

Then, $\mathbf{r}_D = (x_D, 0)$, where $x_D = x - x_P$, and Eq. (6) becomes

$$\ddot{x}_D + 2\mu\dot{x}_D + \mu^2 x_D = 0 \tag{52}$$

which has the solution in Eq. (7). Because the link direction is fixed, the y components of the velocity of the vehicle and the ghost are equal, and so

$$\sin\theta = \dot{s}\cos\zeta \tag{53}$$

The x components of velocity are related by

$$\dot{x}_D = \dot{s}\sin\zeta + \cos\theta = \frac{\cos(\theta - \zeta)}{\cos\zeta} \tag{54}$$

where Eq. (53) has been used. The initial conditions determine $x_D(0)$ from Eq. (52). Also, $x_P = R\cos\zeta$, which determines $\zeta(0)$, whereas the initial direction of Q gives $\theta(0)$. Then, Eq. (54) determines $\dot{x}_D(0)$. Thus, Eq. (52) determines $x_D(\sigma)$ for all σ, and so the x tracking deviation is determined independently of the y motion. Initial conditions $\dot{s}(0) > 0$ and $\theta(0) > 0$ lie in I_+, and the condition in Eq. (17) on μ ensures that the motion converges to anticlockwise tracking of the circle. Taking $s = 0$ when $y = 0$, one has $s(0) = R\zeta(0)$ and $\zeta = s/R$. Then, Eq. (22) becomes

$$\dot{s} = \sqrt{1 - \dot{x}_D^2 \cos^2\frac{s}{R}} + \dot{x}_D \sin\frac{s}{R} \tag{55}$$

which is a (nonautonomous) differential equation for s. The solution and Eq. (53) determine θ. The position of the vehicle is obtained by integrating

$$\dot{x} = \cos\theta \quad \text{and} \quad \dot{y} = \sin\theta \tag{56}$$

The ghost will reach the apex of the circle, at which $\zeta = \pi/2$. Then, Eq. (53) implies $\theta = \pi$, and so $\dot{y} = 0$, which implies that the vehicle path then reaches an apex too. This is evidently necessary for consistent geometry. At this point, one simply has $\dot{s} = 1 - \dot{x}_D$.

Theorem 5 implies that the vehicle path converges to the circle if $\mu > 0$, $|\dot{x}_D(0)| < 1$, and $\mu|x_D(0)| \le 2$. Equation (54) shows that the vehicle path does not converge if $|\dot{x}_D|$ ever exceeds $1/\cos\zeta$. However, ζ involves the absolute motion, and so this does not translate into simple conditions on the initial state.

Figure 8 illustrates the solution for a circle of radius 250 m. The path Q starts at coordinates $(-125,\ 0)$ m at an angle of $\theta = 30$ deg with the x axis. The ghost starts at point (250, 0) m on the circle with $\dot{s} = 0.5$, as Eq. (53) requires. The condition in Eq. (47) shows that convergence will occur if $\mu \le 2/375 = 0.005\dot{3}\ \text{m}^{-1}$. The value chosen is $\mu = 0.005\ \text{m}^{-1}$, and Fig. 8 confirms the convergence. Park et al. [14] considers a vehicle speed of 25 m/s, which would imply a convergence rate of $25\mu = 0.13\ \text{s}^{-1}$, or a time constant of 7.5 s.

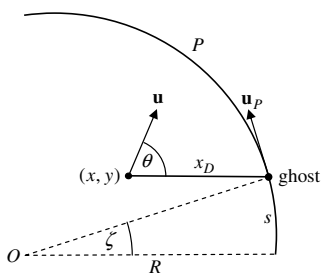

Fig. 7 Variables for the circle tracking solution.

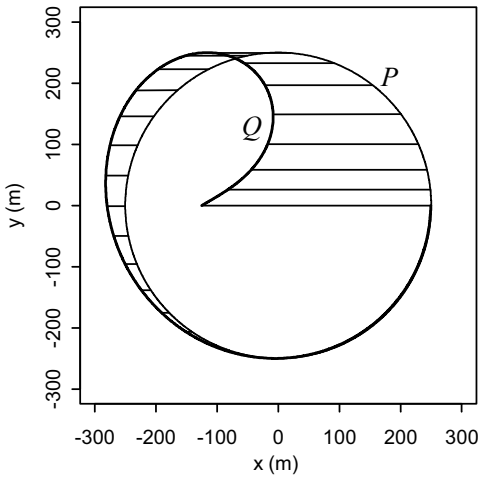

Fig. 8 An example of convergence to a circle in planar motion.

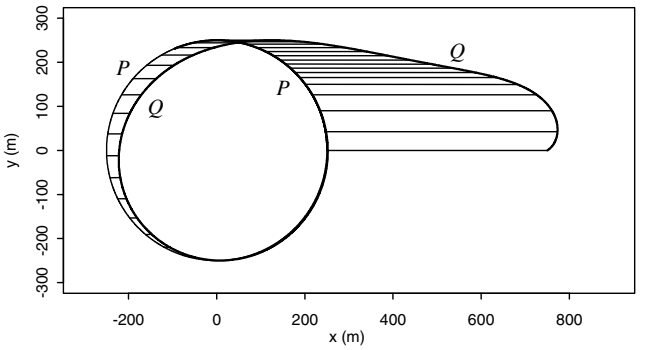

Fig. 9 Another example of convergence to a circle in planar motion.

Figure 9 illustrates the solution with only the initial vehicle position changed to (750, 0) m. Here, Eq. (47) implies convergence if $\mu \le 2/500 = 0.004\ \text{m}^{-1}$, which is the value chosen. The figure again confirms this convergence.

Section X illustrates how these solutions are influenced by limitations on the turn radius of the vehicle. If the motion initially lies on the boundary set I_0 with $\zeta(0) = 0$ and $\theta(0) = 0$, then s remains zero, and so path tracking does not occur.

Other initial directions of the link could be chosen, providing some additional control on the path taken by the vehicle. By contrast, the vector field method [7] determines a unique path to the circle. The method of [14–16] would not converge in these cases, because the initial length of the link exceeds the radius of the circle.

IX. Geometric Equations for Q in Standard Differential Form

Here, the AL guidance Eqs. (2) and (5) for Q are transformed into ordinary differential equations in standard form. This removes the awkward algebraic Eq. (5) and provides a much simpler way of computing Q for a general P. Some examples are given. It will also provide a means of limiting the curvature of the path (Sec. X). The transformed equations are

$$\dot{\mathbf{r}} = \mathbf{u} \tag{57}$$

$$\dot{\mathbf{u}} = \frac{(\mathbf{e}_P \times \bar{\mathbf{G}}) \times \mathbf{u}}{\mathbf{e}_P \cdot \mathbf{u}} \tag{58}$$

$$\dot{s} = \zeta \tag{59}$$

$$\dot{\zeta} = -\frac{\bar{\mathbf{G}} \cdot \mathbf{u}}{\mathbf{e}_P \cdot \mathbf{u}} \tag{60}$$

where

$$\bar{\mathbf{G}} = \zeta^2 \mathbf{e}'_P + \bar{\mathbf{F}} \tag{61}$$

In the kinetic interpretation, ζ is the speed of the ghost and $\dot{\zeta}$ is its axial acceleration. These are eight first-order nonlinear differential equations for $\mathbf{r}$, $\mathbf{u}$, s, and ζ in standard form. To derive the equations, we restate Eq. (2) as

$$\dot{\mathbf{u}} = \dot{\mathbf{u}}_P + \bar{\mathbf{F}} \tag{62}$$

From Eq. (4)

$$\dot{\mathbf{u}}_P = \dot{\zeta}\mathbf{e}_P + \zeta\dot{\mathbf{e}}_P = \dot{\zeta}\mathbf{e}_P + \zeta^2\mathbf{e}'_P \tag{63}$$

Writing Eq. (5) in the form $\mathbf{u} \cdot \mathbf{u} = 1$ and differentiating gives $\dot{\mathbf{u}} \cdot \mathbf{u} = 0$, and so Eq. (62) gives

$$0 = \dot{\mathbf{u}}_P \cdot \mathbf{u} + \bar{\mathbf{F}} \cdot \mathbf{u} = \dot{\zeta}\mathbf{e}_P \cdot \mathbf{u} + \bar{\mathbf{G}} \cdot \mathbf{u} \tag{64}$$

which gives Eq. (60). Then, Eqs. (62) and (63) give

$$\dot{\mathbf{u}} = \bar{\mathbf{G}} + \dot{\zeta}\mathbf{e}_P = \bar{\mathbf{G}} - \frac{\bar{\mathbf{G}} \cdot \mathbf{u}}{\mathbf{e}_P \cdot \mathbf{u}}\mathbf{e}_P \tag{65}$$

which gives Eq. (58).

The reduction depends on the assumption that $\mathbf{e}_P \cdot \mathbf{u} \neq 0$, which is satisfied in the sets I_+ and I_- but excludes the boundary set I_0. The essential idea behind the previous transformations is as follows. Equations (62) and (63) comprise four differential equations for $\dot{\zeta}$ and the three components of $\dot{\mathbf{u}}$, forming a composite system with a 4×4 matrix of coefficients. The method effectively inverts the matrix to obtain $\dot{\zeta}$ and $\dot{\mathbf{u}}$ explicitly.

Equation (58) ensures that $\mathbf{u}$ remains a unit vector if it is initially so. Thus, the constraint in Eq. (5) is no longer required. Hence, both $\mathbf{r}$ and $\mathbf{u}$ can be expressed in Cartesian coordinates, which is convenient for solving Eqs. (57–60) numerically. The initial values $\mathbf{r}$ and $\mathbf{u}$ are given, whereas initial values of s and ζ must be chosen. They can be chosen, according to Theorem 6, to obtain the greatest rate of convergence.

Equations (57–60) are very convenient for computing vehicle paths, such as the examples in Figs. 4, 6, and 8, and the following examples. Figures 10 and 11 illustrate nonplanar convergence to the circle of Fig. 8. The path Q starts at position $\mathbf{r}(0) = (100, 0, 200)$ m, which is 200 m above the horizontal circle in the (x, y) plane. The path makes an angle of 30 deg with the x axis, and so $\mathbf{u}(0) = (\sqrt{3}/2, 1/2, 0)$. The ghost starts at the point $\mathbf{r}_P(0) = (250, 0, 0)$ m, and so $|\mathbf{r}_D(0)| = \sqrt{150^2 + 200^2} = 250$ m. Initially, $\dot{s} = 0.5$, and so the projection of the link on the (x, y) plane has a fixed direction. The link itself does have a fixed direction but remains normal to $\mathbf{e}_P(0)$, as described near the end of Sec. VII. Theorem 5 shows that convergence will occur if $\mu \leq 2/250 = 0.008$ m^{-1}. This is used in Figs. 10 and 11, which confirm the convergence. A vehicle speed of 25 m/s would imply a convergence rate of $25\mu = 0.2$ s^{-1}, or a time constant of 5 s. The termination point in Fig. 10 represents 60 s at this speed.

A helical path is convenient for climbing or descending while maintaining horizontal vicinity. Figure 12 illustrates convergence to a defined helix on a vertical cylinder of radius 250 m, having a one-in-five climb or pitch. The initial state of the vehicle and ghost, and the value of μ, are exactly as in the preceding example. One notes the similarity of the initial vehicle trajectory here to that in Fig. 11.

Figure 13 illustrates how the guidance logic can track to an articulated path comprising lines and arcs. It also shows that guidance can direct the vehicle to cross one segment of P and follow another segment. Here, the paths are coplanar, and P involves a U-turn. The vehicle is required to track toward the lower straight line at $y = -100$ from a starting position of $\mathbf{r}(0) = (0, 200)$ m above the upper straight line at $y = 100$. This is achieved by locating the ghost

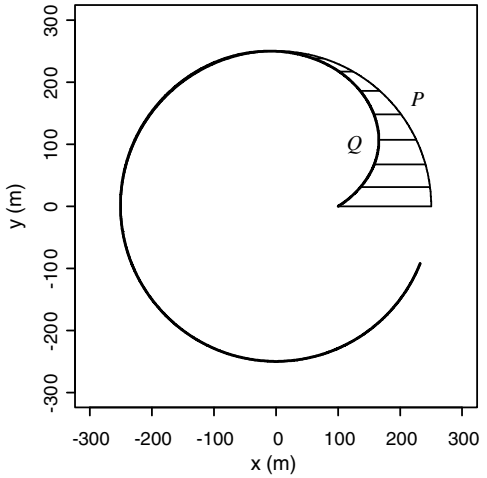

Fig. 10 Plan view of nonplanar convergence to a circle.

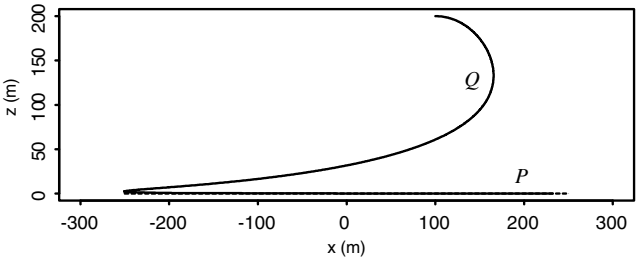

Fig. 11 Side view of nonplanar convergence to a circle.

initially at $\mathbf{r}_P(0) = (0, -100)$ m. The straight lines extend for 500 m and are linked by a semicircle of radius 100 m. The vehicle path Q is initially parallel to the x axis, and so $\mathbf{u}(0) = (1, 0)$. Initially, $\dot{s} = 1$, and so the link has a fixed direction. Theorem 2 shows that convergence occurs if $\mu \leq e/300 = 0.00906$ m^{-1}. The value $\mu = 0.008$ m^{-1} is used in Fig. 13, which confirms the convergence. A vehicle speed of 25 m/s would imply a convergence rate of $25\mu = 0.2$ s^{-1}, or a time constant of 5 s.

The method of [14–16] could not produce such convergence, because it would require a link of a length greater than 300 m to track to the lower arm, but a link of a length less than 100 m to track the circle. The vector field method [7] would be complicated, because the vehicle initially lies in the field of the upper arm of the U. The switching on and off of fields would have to be carefully managed.

X. Curvature Limits on Vehicle Capability

This section considers the effects of placing a limit K on the curvature of Q, which is a typical practical limit for real vehicles. For

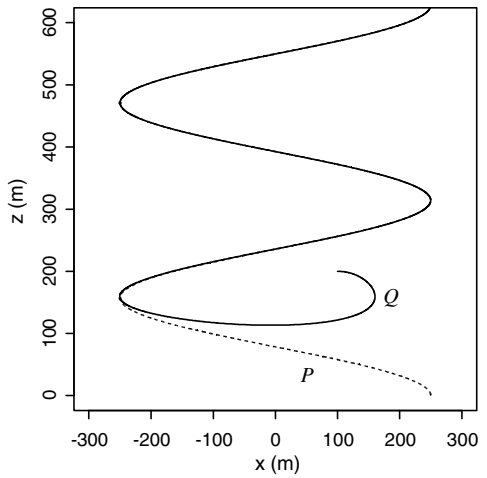

Fig. 12 Side view in the y direction of convergence to a helix.

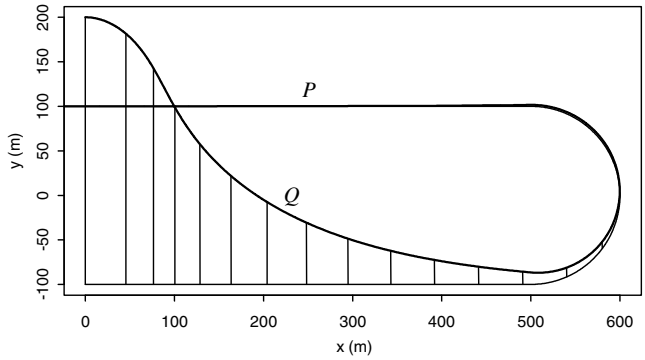

Fig. 13 Convergence to a U-shaped path across one arm of the U.

an aircraft (for example), K will depend on the speed and air density, hence on altitude and temperature. It will also depend on the plane in which the turn occurs, because vertical turns have different limits from horizontal turns. However, to simplify matters, we suppose here that the absolute curvature κ of Q is bounded; thus,

$$\kappa \le K \tag{66}$$

First, this must be satisfied in the steady state, and so it is necessary that the curvature κ_P of P satisfies $\kappa_P \le K$. Second, it is fairly clear from Theorem 1 that, provided $|\dot{\mathbf{r}}_D(0)| < 1$, one can satisfy Eq. (66) and achieve convergence by choosing a small enough μ, because $\kappa \to 0$ as $\mu \to 0$. If $|\dot{\mathbf{r}}_D(0)|$ is not close to 1 and κ_P is not close to K, then a larger μ can be chosen. Here, we estimate how large μ can be. As

$$|\dot{\mathbf{u}}| = \kappa \tag{67}$$

we need to bound $|\dot{\mathbf{u}}|$. Equation (58) for $\dot{\mathbf{u}}$ involves $\bar{\mathbf{G}}$, which can be written as

$$\bar{\mathbf{G}} = \zeta^2 \kappa_P \mathbf{n}_P + \bar{\mathbf{F}} \tag{68}$$

where $\mathbf{n}_P$ is the inward normal on the osculating plane [22]. Then, Eq. (58) implies

$$|\dot{\mathbf{u}}| \le \frac{|\bar{\mathbf{G}}|}{|\mathbf{u} \cdot \mathbf{e}_P|} \le \frac{\zeta^2 \kappa_P + |\bar{\mathbf{F}}|}{|\mathbf{u} \cdot \mathbf{e}_P|} \tag{69}$$

Bounds obtained previously, for the purpose of proving convergence, merely ensure that $|\mathbf{u} \cdot \mathbf{e}_P|$ does not fall to zero. For the present purpose, one evidently needs to bound $\mathbf{u} \cdot \mathbf{e}_P$ well away from zero. First, Eq. (20) implies

$$|\mathbf{u} \cdot \mathbf{e}_P| \ge \sqrt{1 - |\dot{\mathbf{r}}_D|^2} \tag{70}$$

because $|\dot{\mathbf{r}}_D \times \mathbf{e}_P| \le |\dot{\mathbf{r}}_D|$. To bound $|\dot{\mathbf{r}}_D|$ well away from 1, consider the energy function:

$$E = \mu^2 |\mathbf{r}_D|^2 + |\dot{\mathbf{r}}_D|^2 \tag{71}$$

The first term represents the elastic energy in the fictitious spring. The second represents the kinetic energy of the vehicle (of notional mass 2) in the frame of reference moving with the ghost. Using Eq. (6), we get

$$\dot{E} = 2\mu^2 \mathbf{r}_D \cdot \dot{\mathbf{r}}_D + 2\dot{\mathbf{r}}_D \cdot \ddot{\mathbf{r}}_D = -4\mu |\dot{\mathbf{r}}_D|^2 \le 0 \tag{72}$$

The Dirichlet conditions and the differential equations imply that $\dot{\mathbf{r}}_D$ is continuous, and so $\dot{E}$ is continuous (i.e., it exists), even though $\dot{\mathbf{u}}$ and $\ddot{s}$ could have discontinuities. Then, we have

$$|\dot{\mathbf{r}}_D|^2 \le E(\sigma) \le E(0) \tag{73}$$

and so Eq. (70) implies

$$|\mathbf{u} \cdot \mathbf{e}_P| \ge \sqrt{1 - E(0)} \tag{74}$$

Incidentally, the decrease of E shows that a set $\{\Xi\colon E < c\}$ is invariant for any constant c. Now, suppose that

$$\mu |\mathbf{r}_D(0)| \le \sqrt{1 - |\dot{\mathbf{r}}_D(0)|^2} \tag{75}$$

which evidently confines μ to smaller values than those admitted by the convergence condition in Eq. (47). Then, $E(0) < 1$, and so Eq. (74) provides a real bound. Next, we bound the numerator of Eq. (69). From Eq. (22),

$$|\zeta| = |\dot{s}| \le |\mathbf{u} \cdot \mathbf{e}_P| + |\dot{\mathbf{r}}_D \cdot \mathbf{e}_P| \le 1 + |\dot{\mathbf{r}}_D| \le 1 + \sqrt{E(0)} \tag{76}$$

Also, Eq. (71) implies

$$|\mathbf{r}_D|^2 \le E(\sigma)/\mu^2 \le E(0)/\mu^2 \tag{77}$$

and so

$$|\bar{\mathbf{F}}| \le 2\mu |\dot{\mathbf{r}}_D| + \mu^2 |\mathbf{r}_D| \le 3\mu \sqrt{E(0)} \tag{78}$$

Combining Eqs. (67), (69), (74), and (78), one obtains

$$\kappa \le \frac{[1 + \sqrt{E(0)}]^2 \kappa_P + 3\mu \sqrt{E(0)}}{\sqrt{1 - E(0)}} \tag{79}$$

This limits $\kappa(\sigma)$ at each point σ of Q in terms of $\kappa_P(s)$ at the linked point $s(\sigma)$ of P. With Eq. (66), this puts an upper limit on the current choice of μ. Suppose the largest curvature on P is $\bar{\kappa}_P$, and define

$$b(\mu) = \sqrt{E(0)} < 1 \tag{80}$$

and

$$f(\mu) = 3\mu b(\mu) + [1 + b(\mu)]^2 \bar{\kappa}_P - \sqrt{1 - b(\mu)^2} K \tag{81}$$

Then, Eq. (79) implies that Eq. (66) holds for all σ if

$$f(\mu) < 0 \tag{82}$$

Evidently, $f(\mu) \uparrow$ as $\mu \uparrow$, and so Eq. (82) implies $\mu < \bar{\mu}$ for the unique $\bar{\mu}$, satisfying $f(\bar{\mu}) = 0$. Also, $f(\mu) \uparrow$ as $\bar{\kappa}_P \uparrow$. Hence, $\bar{\mu} \downarrow$ as $\bar{\kappa}_P \uparrow$, and so a smaller μ is required for defined paths of greater curvature, as expected. A positive $\bar{\mu}$ is possible only if $f(0) < 0$, which places an upper limit on $\bar{\kappa}_P$ for these estimates to be useful:

$$\bar{\kappa}_P < \frac{\sqrt{1 - D^2}}{(1 + D)^2} K \tag{83}$$

where $D = |\dot{\mathbf{r}}_D(0)|$ is the initial divergence rate. In the following examples, a miniature UAV has the speed $V = 25$ m/s, as in [14], and a turning limit of $K = 1/50$ m^{-1}, say, at this speed.

Example 1. P is a straight line. The UAV is initially on the defined path, and so $\mathbf{r}_D(0) = \mathbf{0}$ but is diverging from the path at rate 10 m/s. The divergence rate (per unit distance σ along Q) is $D = 10/25 = 0.4$. Then, Eq. (80) gives $b = D$, and Eq. (82) becomes

$$\mu < \frac{K}{3b} \sqrt{1 - D^2} = 0.0153 \text{ m}^{-1} \tag{84}$$

The time constant for convergence is $1/\mu V = 2.6$ s. Here, the condition Eq. (75) does not limit μ. The initial state implies that Q remains coplanar with P.

Example 2. P is a straight line. The UAV is initially $|\mathbf{r}_D(0)| = 100$ m from the path and not diverging, and so $D = 0$. Then, $b = \mu |\mathbf{r}_D(0)|$, and the equation $f(\bar{\mu}) = 0$ reduces to a quadratic equation for $\bar{\mu}^2$. The solution gives $\bar{\mu} = 0.00692$ s^{-1}, or a time constant of 5.8 s. The condition in Eq. (75) requires only $\mu < 0.01$ m^{-1}, which does not constrain μ further. The initial state does not constrain Q to be coplanar with P.

Example 3. P is a circle of radius 250 m, as in [14], and so $\bar{\kappa}_P = 1/250$ m^{-1}. For the initial conditions of example 1, Eq. (82) becomes

$$\mu < \frac{1}{3b}[\sqrt{1-D^2}K - (1+D)^2\bar{\kappa}_P] = 0.00874 \text{ m}^{-1} \tag{85}$$

or a time constant exceeding 4.6 s. Again, the condition in Eq. (75) does not limit μ. Here, Eq. (83) shows that the estimates do not yield a positive $\bar{\mu}$ unless the radius of the defined circle exceeds 107 m. The initial state does not constrain Q to be coplanar with P.

Example 4. P is a circle of radius 250 m. For the initial conditions of example 2, solving $f(\bar{\mu}) = 0$ numerically gives $\bar{\mu} = 0.00516 \text{ m}^{-1}$, or a time constant exceeding 7.8 s. Again, Eq. (75) does not constrain μ further. The initial state does not constrain Q to be coplanar with P. The estimate of $\bar{\mu}$ does not depend on whether the vehicle is initially inside or outside the circle.

The bounds used in Eqs. (69–82) are not tight, and so the calculated $\bar{\mu}$ is often smaller than is really required. The bounds have the merit of not being very sensitive to the details of P or to the initial configuration, as example 4 shows.

In the method of [16], the considerations for constraining κ are somewhat different. There, the fixed length of the link is constrained by the scenario, and so it is natural to supplement guidance by a curvature limit, in which turning occurs at the constant κ. In AL guidance, there are no such constraints on the rate parameter μ, and so it is natural to use the turning limit to constrain μ.

XI. Kinetic Equations in a Fixed or Moving Medium

The simplest vehicle motion along the path Q is a constant speed V, this being the ground speed (or inertial speed). For an aircraft in level motion in still air, this is approximately feasible and, likewise, for a watercraft in the absence of a current or wind. In this case, the geometric Eqs. (57–60) are easily transformed into kinetic equations by substituting the time t for the distance $\sigma = Vt$. These will be stated later.

In a moving medium, a vehicle (such as an aircraft) knows its ground velocity $\mathbf{V}$ from its INS–GPS system, and it can measure its velocity $\mathbf{U}$ (relative to the medium) using onboard systems. They are related by $\mathbf{V} = \mathbf{U} + \mathbf{W}$, where $\mathbf{W}(\mathbf{r}, t)$ is the velocity field of the medium. For an aircraft, $\mathbf{W}$ is the wind (or air mass) velocity. In practice, $\mathbf{W}$ might not be accurately known by the vehicle, especially in a turbulent medium. Only limited information about $\mathbf{W}$ might be available from fixed monitoring stations. More sophisticated navigation systems can often infer $\mathbf{W}$. However, the guidance law does not require a knowledge of $\mathbf{W}$. For a watercraft in still air, $\mathbf{W}$ is the velocity of the water current. The additional effects of wind on a watercraft are more complex, and they are beyond the scope of this paper. The following mathematics admit a general field $\mathbf{W}$. In a real vehicle, the measurement of $\mathbf{U}$ and its alignment with the vehicle might be problematic if $\mathbf{W}$ is too variable.

We suppose that the vehicle travels at the fixed relative speed $U = |\mathbf{U}|$. For an aircraft, U is the airspeed, which is often fairly constant. Then, $\mathrm{d}\mathbf{V}/\mathrm{d}t$ is normal to $\mathbf{U}$. Also, $\mathbf{V} = V\mathbf{u}$, but the ground speed V is not constant in a moving medium. The speed of the ghost is denoted by w. The resulting differential equations in the kinetic state variables $\mathbf{r}$, $\mathbf{V}$, s, and w, are

$$\frac{\mathrm{d}\mathbf{r}}{\mathrm{d}t} = \mathbf{V} \tag{86}$$

$$\frac{\mathrm{d}\mathbf{V}}{\mathrm{d}t} = \frac{(\mathbf{V}\times\mathbf{H}\times\mathbf{V})\times\mathbf{U}}{\mathbf{V}\cdot\mathbf{U}} \tag{87}$$

$$\frac{\mathrm{d}s}{\mathrm{d}t} = w \tag{88}$$

$$\frac{\mathrm{d}w}{\mathrm{d}t} = w\frac{\mathbf{V}\cdot\mathbf{H}\times\mathbf{U}}{\mathbf{V}\cdot\mathbf{U}} - J \tag{89}$$

where

$$\mathbf{H} = \frac{\mathbf{e}_P\times\mathbf{G}}{\mathbf{e}_P\cdot\mathbf{V}} \tag{90}$$

and

$$J = \frac{\mathbf{G}\cdot\mathbf{V}}{\mathbf{e}_P\cdot\mathbf{V}} \tag{91}$$

Here

$$\mathbf{G} = V^2\bar{\mathbf{G}} = w^2\mathbf{e}'_P + \mathbf{F} \tag{92}$$

and

$$\mathbf{F} = V^2\bar{\mathbf{F}} = -\lambda^2\mathbf{r}_D - 2\lambda\frac{\mathrm{d}\mathbf{r}_D}{\mathrm{d}t} \tag{93}$$

and $\lambda = V\mu$, which is not constant if V varies. Now, $\mathbf{F}$ has the dimensions of force and λ the dimensions of frequency, and so the kinetic meaning is more direct. The equations are derived as follows. The ground speed is $V = \mathrm{d}\sigma/\mathrm{d}t$. Differentiating the ground velocity $\mathbf{V} = V\mathbf{u}$ gives

$$\frac{\mathrm{d}\mathbf{V}}{\mathrm{d}t} = \frac{\mathrm{d}V}{\mathrm{d}t}\mathbf{u} + V^2\dot{\mathbf{u}} \tag{94}$$

Because this is normal to $\mathbf{U}$, its scalar product with $\mathbf{U}$ gives

$$\frac{\mathrm{d}V}{\mathrm{d}t} = -V^2\frac{\dot{\mathbf{u}}\cdot\mathbf{U}}{\mathbf{u}\cdot\mathbf{U}} \tag{95}$$

Putting this in Eq. (94) gives

$$\frac{\mathrm{d}\mathbf{V}}{\mathrm{d}t} = \frac{V^2}{\mathbf{V}\cdot\mathbf{U}}(\mathbf{V}\times\dot{\mathbf{u}})\times\mathbf{U} \tag{96}$$

This formula can also be used in simulations or, if $\mathbf{W}$ is known, by replacing $\mathbf{U}$ by $\mathbf{V} - \mathbf{W}$. Because $\mathbf{G} = V^2\bar{\mathbf{G}}$, Eq. (58), can be written as $V^2\dot{\mathbf{u}} = \mathbf{H}\times\mathbf{V}$. Putting this in Eq. (96) gives Eq. (87).

The speed of the ghost is $w = V\zeta$. Equation (60) may be written as $\dot{\zeta} = -J$. Thus, we get

$$\frac{\mathrm{d}w}{\mathrm{d}t} = \zeta\frac{\mathrm{d}V}{\mathrm{d}t} + V\frac{\mathrm{d}\zeta}{\mathrm{d}t} = \frac{w}{V}\frac{\mathrm{d}V}{\mathrm{d}t} - J \tag{97}$$

Differentiating $V^2 = \mathbf{V}\cdot\mathbf{V}$ and using Eq. (87), one gets

$$\frac{1}{V}\frac{\mathrm{d}V}{\mathrm{d}t} = \frac{\mathbf{V}}{V^2}\cdot\frac{\mathrm{d}\mathbf{V}}{\mathrm{d}t} = \frac{\mathbf{V}\cdot\mathbf{H}\times\mathbf{U}}{\mathbf{V}\cdot\mathbf{U}} \tag{98}$$

Putting this in Eq. (97) gives Eq. (89), which completes the derivation of Eqs. (86–89).

The equations can easily be solved numerically using Cartesian components for both $\mathbf{r}$ and $\mathbf{V}$, because there are no constraints. The command acceleration is given by Eq. (87), but this involves s and w. Thus, its value is not known explicitly in terms of the current state variables $\mathbf{r}$ and $\mathbf{V}$. The vehicle needs to compute the acceleration by incrementing the differential equations to find the current values of the ghost variables s and w. This is similar to the method of [14–16], in which the location of the reference point must be determined incrementally in order to compute the command acceleration.

For a fixed medium, we set $\mathbf{U} = \mathbf{V}$ in Eqs. (87) and (89), which reduce to

$$\frac{\mathrm{d}\mathbf{V}}{\mathrm{d}t} = \mathbf{H}\times\mathbf{V} \tag{99}$$

$$\frac{\mathrm{d}w}{\mathrm{d}t} = -J \tag{100}$$

Now, V and λ are constant. As mentioned, these equations can easily be obtained directly from Eqs. (58) and (60) by substituting $\sigma = Vt$.

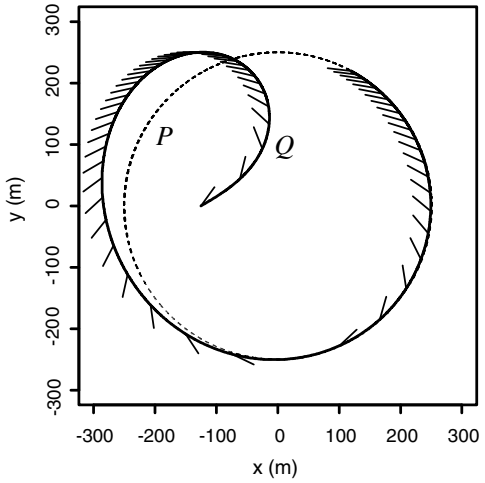

Fig. 14 Convergence to a circle in planar motion in a medium moving in the x direction. The path is identical to that shown in Fig. 8.

Figure 14 illustrates a circle tracking simulation with the same parameters as those used in Fig. 8, except that the vehicle now has a fixed speed $U = 25$ m/s relative to the medium, and there is a strong wind or current in the x direction with speed $W = 20$ m/s. The duration is 130 s. The path is identical to that shown in Fig. 8, confirming that the path is independent of the motion of the medium. The whiskers indicate the direction of **U** at 2 s intervals, and so the spacing indicates ground speed V. This varies between 5 m/s, when heading against the current, to 45 m/s, when heading along the current. The whiskers would also indicate the direction of the body axis of an ideal vehicle in the absence of pitch or yaw.

XII. Conclusions

A new guidance logic for a vehicle tracking exactly toward a defined path of any smooth, 3-D shape has been formulated and shown to have good convergence properties. Some recent methods track exactly only to straight paths and circles in planar motion. Kinetic equations and command accelerations have been formulated for constant relative speed in a moving medium. This includes a constant speed in a fixed medium as a special case. These are reasonable assumptions for water surface vehicles and for aerial vehicles in level flight. They are also reasonable for an aerial vehicle in a steady climb or descent angle, including a helical path. For more general paths, one could consider speed variations consistent with vehicle performance and gravity.

The new method is more complex, in some ways, than a previous method based on a moving reference point. In general, it results in one more differential equation. However, in the case of a straight line and a circle, the new solutions are simpler.

In a fixed medium, limits on vehicle turning capability have been used to limit the convergence rate parameter. There is scope for refining these estimates, extending them to a moving medium, and allowing for different limits on horizontal and vertical turning capability. One could also investigate the effects of turning at the constant curvature limit, when the command curvature exceeds this value.

Acknowledgments

The author thanks N. L. Fulton and M. Westcott for helpful discussions and J. Deyst, J. P. How, and S. Park for helpful correspondence.

References

[1] Franklin, G. E., Powell, J. D., and Emami-Naeini, A., *Feedback Control of Dynamic Systems*, 4th ed., Prentice–Hall, Upper Saddle River, NJ, 2002.

[2] Keviczky, T., and Balas, G. J., "Software Enabled Flight Control Using Receding Horizon Techniques," AIAA Guidance, Navigation, and Control Conference and Exhibit, AIAA Paper 2003-5671, Aug. 2003.

[3] Murray, R. M., "Trajectory Generation for a Towed Cable System Using Differential Flatness," *Proceedings of the 13th World Congress: International Federation of Automatic Control*, Pergamon, Oxford, U.K., 1997, pp. 395–400.

[4] Rathinam, M., and Murray, R. M., "Configuration Flatness of Lagrangian Systems Underactuated by One Control," *SIAM Journal on Control and Optimization*, Vol. 36, No. 1, 1998, pp. 164–179. doi:10.1137/S0363012996300987

[5] Johnson, E., Calise, A., and Corban, E., "A Six Degree-of-Freedom Adaptive Flight Control Architecture for Trajectory Following," AIAA Guidance, Navigation, and Control Conference and Exhibit, AIAA Paper 2002-4776, Aug. 2002.

[6] Niculescu, M., "Lateral Track Control for Aerosonde UAV," 39th AIAA Aerospace Sciences Meeting and Exhibit, AIAA Paper 2001-6575, Jan. 2001.

[7] Nelson, D. R., Barber, D. B., McLain, T. W., and Beard, R. W., "Vector Field Path Following for Miniature Air Vehicles," *IEEE Transactions on Robotics and Automation*, Vol. 23, No. 3, June 2007, pp. 519–529. doi:10.1109/TRO.2007.898976

[8] Lawrence, D. A., Frew, E. W., and Pisano, W. J., "Lyapunov Vector Fields for Autonomous Unmanned Aircraft Flight Control," *Journal of Guidance, Control, and Dynamics*, Vol. 31, No. 5, Sept.–Oct. 2008, pp. 1220–1229. doi:10.2514/1.34896

[9] Amidi, O., and Thorpe, C., "Integrated Mobile Robot Control," *Proceedings of SPIE: The International Society for Optical Engineering*, Vol. 1388, No. 504, March 1991, pp. 505–523.

[10] Ollero, A., and Heredia, G., "Stability Analysis of Mobile Robot Path Tracking," *Proceedings of the Institute of Electrical and Electronics Engineers/Robotics Society of Japan International Conference on Intelligent Robot Systems*, IEEE Publications, Piscataway, NJ, 1995, pp. 461–466.

[11] Murphy, K. N., "Analysis of Robotic Vehicle Steering and Controller Delay," *5th International Symposium on Robotics and Manufacturing (ISRAM)*, American Society of Mechanical Engineers, New York, 1994, pp. 631–636.

[12] Rankin, A. L., Crane, C. D., and Armstrong, D., "Evaluating a PID, Pure Pursuit, and Weighted Steering Controller for an Autonomous Land Vehicle," *Proceedings of SPIE: The International Society for Optical Engineering*, Vol. 3210, Jan. 1998, pp. 1–12. doi:10.1117/12.299554

[13] Hogg, R., Rankin, A., Roumeliotis, S., McHenry, M., Helmick, D., Bergh C., and Matthies, L., "Algorithms and Sensors for Small Robot Path Following," *Institute of Electrical and Electronics Engineers International Conference on Robotics and Automation*, Vol. 4, IEEE Publications, Piscataway, NJ, 2002, pp. 3850–3857.

[14] Park, S., Deyst, J., and How, J. P., "A New Nonlinear Guidance Logic for Trajectory Tracking," AIAA Guidance, Navigation, and Control Conference, AIAA Paper 2004-4900, Aug. 2004.

[15] Deyst, J., How, J. P., and Park, S., "Lyapunov Stability of a Nonlinear Guidance Law for UAVs," AIAA Atmospheric Flight Mechanics Conference and Exhibit, AIAA Paper 2005-6230, Aug. 2005.

[16] Park, S., Deyst, J., and How, J. P., "Performance and Lyapunov Stability of a Nonlinear Path-Following Guidance Method," *Journal of Guidance, Control, and Dynamics*, Vol. 30, No. 6, Nov.–Dec. 2007, pp. 1718–1728. doi:10.2514/1.28957

[17] Frazzoli, E., Mao, Z.-H., Oh, J.-H., and Feron, E., "Resolution of Conflicts Involving Many Aircraft via Semi-Definite Programming," *Journal of Guidance, Control, and Dynamics*, Vol. 24, No. 1, Jan.–Feb. 2001, pp. 79–86. doi:10.2514/2.4678

[18] Tomlin, C., Mitchell, I., and Ghosh, R., "Safety Verification of Conflict Resolution Manoeuvres," *IEEE Transactions on Intelligent Transport Systems*, Vol. 2, No. 2, June 2001, pp. 110–120. doi:10.1109/6979.928722

[19] Hu, J., Prandini, M., and Sastry, S., "Optimal Coordinated Maneuvers for Three-Dimensional Aircraft Conflict Resolution," *Journal of Guidance, Control, and Dynamics*, Vol. 25, No. 5, Sept.–Oct. 2002, pp. 888–900. doi:10.2514/2.4982

[20] Sultan, C., and Seereram, S., "Energy Suboptimal Collision-Free Reconfiguration for Spacecraft Formation Flying," *Journal of Guidance, Control, and Dynamics*, Vol. 29, No. 1, Jan.–Feb. 2006, pp. 190–192. doi:10.2514/1.10781

[21] Slater, G. L., Byram, S. M., and Williams, T. W., "Collision Avoidance

for Satellites in Formation," *Journal of Guidance, Control, and Dynamics*, Vol. 29, No. 5, Sept.–Oct. 2006, pp. 1140–1146. doi:10.2514/1.16812

[22] Struik, D. J., *Lectures on Classical Differential Geometry*, 2nd ed., Dover, New York, 1988, pp. 10, 13, 29.

[23] Ascher, U., and Petzold, L., *Computer Methods for Ordinary Differential Equations and Differential-Algebraic Equations*, SIAM Press, Philadelphia, 1998.

[24] Rudin, W., *Principles of Mathematical Analysis*, 2nd ed., McGraw–Hill, New York, 1965, pp. 124, 181.